



Application of a Diffusion Charger for the Measurement of Particle Surface Concentration in Different Environments

Leonidas Ntziachristos , Andrea Polidori , Harish Phuleria , Michael D. Geller & Constantinos Sioutas

To cite this article: Leonidas Ntziachristos , Andrea Polidori , Harish Phuleria , Michael D. Geller & Constantinos Sioutas (2007) Application of a Diffusion Charger for the Measurement of Particle Surface Concentration in Different Environments, Aerosol Science and Technology, 41:6, 571-580, DOI: [10.1080/02786820701272020](https://doi.org/10.1080/02786820701272020)

To link to this article: <http://dx.doi.org/10.1080/02786820701272020>



Published online: 16 May 2007.



Submit your article to this journal [↗](#)



Article views: 479



View related articles [↗](#)



Citing articles: 33 View citing articles [↗](#)



Application of a Diffusion Charger for the Measurement of Particle Surface Concentration in Different Environments

Leonidas Ntziachristos, Andrea Polidori, Harish Phuleria, Michael D. Geller, and Constantinos Sioutas

Department of Civil and Environmental Engineering, University of Southern California, Los Angeles, California, USA

Particle surface area has recently been considered as a possible metric in an attempt to correlate particle characteristics with health effects. In order to provide input to such studies, two Nanoparticle Surface Area Monitors (NSAMs, TSI, Inc.) were deployed in different urban sites within Los Angeles to measure the concentration levels and the diurnal profiles of the surface area of ambient particles. The NSAM's principle of operation is based on the unipolar diffusion charging of particles. Results show that the particle surface concentration decreases from $\sim 150 \mu\text{m}^2 \text{cm}^{-3}$ next to a freeway to $\sim 100 \mu\text{m}^2 \text{cm}^{-3}$ at 100 m downwind of the freeway, and levels decline to $50\text{--}70 \mu\text{m}^2 \text{cm}^{-3}$ at urban background sites. Up to 51% and 30% of the total surface area corresponded to particles $< 40 \text{ nm}$ next to the freeway and at an urban background site, respectively. The NSAM signal was well correlated with a reconstructed surface concentration based on the particle number size distribution measured with collocated Scanning Mobility Particle Sizers (SMPSs, TSI, Inc.). In addition, the mean surface diameter calculated by combination of the NSAM and the total particle number concentration measured by a Condensation Particle Counter (CPC, TSI, Inc.) was in reasonable agreement with the arithmetic mean SMPS diameter, especially at the urban site. This study corroborates earlier findings on the application of diffusion chargers for ambient particle monitoring by demonstrating that they can be effectively used to monitor the particle surface concentration, or

combined with a CPC to derive the mean surface diameter with high temporal resolution.

1. INTRODUCTION

An increasing body of scientific evidence suggests that the surface concentration of inhaled particles may be a suitable metric for the association of particulate matter (PM) with observed health effects. Tran et al. (2005) showed that the level of inflammation by different dusts in the lungs of rats could be better explained when the lung burden was expressed as total particle surface area instead of PM mass. Brown et al. (2001) found that ultrafine particles caused more inflammation, expressed as increased protein and lactate dehydrogenase in bronchoalveolar lavage, than the same mass of fine particles when instilled into rat lungs. In addition, inflammation was highly correlated with the total surface of the particles instilled. These results were further supported by the study of Elder et al. (2005) who showed that particle surface area is an important parameter affecting inflammatory and histopathological effects of inhaled particles on the lung tissue of rats. Oberdörster (2001) suggested that aerosol surface chemistry appears to play an important role in ultrafine particle toxicity, more so than any other mechanistic pathway for interaction of particles with lung cells. More recently, Stoeger et al. (2006) demonstrated that the PM surface area concentration was best correlated with lung cell inflammation in mice when they were exposed to six different vehicle exhaust-like aerosols. The correlation of health effects with surface area was more significant than the correlation with either particle size or organic carbon content at the same mass dosage. In addition to the above animal toxicology studies, at least two studies have associated human health effects with variables related to surface area. In Atlanta, the geometric surface area of particles in the 10–100 nm diameter range has been associated with acute respiratory visits to an ambulatory medical facility (Sinclair and Tolsma 2004). In a study of Austrian school children, the particle surface concentration measured with a diffusion charger has been associated with lung function and pulmonary symptoms (Moshhammer and Neuberger 2003). The above studies indicate

Received 24 June 2006; accepted 9 February 2007.

This research was supported by the Southern California Particle Center (SCPC), funded by EPA under the STAR program through Grant RD-8324-1301-0 to the University of Southern California and was also supported by the NIEHS-NIH grant no. ES-12243 and the California Air Resources Board (CARB) contract no. 03-329. We would also like to thank Dr. Manisha Singh (TSI Inc.) for availing the NSAM monitors and her assistance with the operation of these instruments. The research described herein has not been subjected to the EPA required peer and policy review and therefore does not necessarily reflect the views of the agency, and no official endorsement should be inferred. Mention of trade names or commercial products does not constitute an endorsement or recommendation for use.

Address correspondence to Constantinos Sioutas, University of Southern California, Department of Civil and Environmental Engineering, 3620 S. Vermont Avenue, Los Angeles, CA 90089, USA. E-mail: sioutas@usc.edu

that the surface concentration of ambient particles in different environments may be a very useful PM property in our efforts to associate health effects with exposure.

The quantification of particle surface area from ambient samples depends on the instrument used because the variable chemical character (organic or elemental carbon, crustal materials, salts, etc.) and morphology (agglomerates, volatile droplets, etc.) of particles affect the instrument's response. Instruments that have been used so far include the photoelectric aerosol sensor (PAS), the epiphaniometer, and different models of diffusion chargers. In the PAS (Matter et al. 1999), particles are irradiated with ultraviolet light and photoelectrons are emitted from the particle surface, which then becomes positively charged. The particle charge is determined by an electrometer after particle collection on a filter. PAS response largely depends on the surface chemistry and it is mainly used for qualitative characterization of aerosol concentrations. In the epiphaniometer (Gäggeler et al. 1989) radioactive lead atoms attach to particles by diffusion. The particles are then collected on a filter and the "Fuchs" surface area (Pandis et al. 1991) is determined by measuring the α -activity of the attached atoms. The "Fuchs" surface corresponds to the epiphaniometer signal (neglecting particle losses in the instrument) and is directly proportional to the particle surface area that is available for diffusion. This is a particularly useful PM metric because it corresponds to the actual particle surface area exposed to the environment and can be used to quantify, for example, the area available for adsorption of gaseous species or for interaction with the epithelial tissue in the lungs. In diffusion chargers, ions instead of atoms attach onto the particles. Rogak and Flagan (1992) showed that the probability for ion attachment scaled with the projected area of a particle, which, for low fractal dimension aggregates, scales with the total particle surface area. Therefore, the use of ion instead of neutral molecule diffusion is also acceptable to determine particle surface. However, the surface area for ionic diffusion is slightly different than the Fuchs surface due to electrical forces (image forces for particles with $Kn \gg 1$ and repulsion forces for particles in the continuum regime— $Kn < \sim 0.2$) as well as the ion tendency to form clusters that may change their mean free path, depending on the carrier gas humidity (Pui et al. 1988). To differentiate the two, Siegmann and Siegmann (2000) used the term "active" to characterize the surface area recorded by diffusion chargers. Ntziachristos et al. (2004) showed that, for practical applications with polydisperse aerosols in the size range found in the atmosphere (10–300 nm), there is a small difference between the so-called "active" and the Fuchs surface metrics. In addition, diffusion chargers have the advantage of providing much faster response (\sim s) compared to the epiphaniometer (\sim 30 min). Therefore, the diffusion charger signal can be used as a quasi real-time measure of the particle surface concentration.

Diffusion chargers have been used in the past to characterize ambient aerosols. Bukowiecki et al. (2002) combined a diffusion charger, a PAS and a CPC to derive a mean surface-weighted particle diameter, and they used the information on the particle

surface properties to study aerosol ageing in the atmosphere. Woo et al. (2001) used a diffusion charger together with a mass concentration monitor and a CPC to reconstruct ambient particle size distributions based on two moments of particle diameter and the particle number concentration, respectively. Imhof et al. (2005) utilized a diffusion charger, a CPC, and a NO_x analyzer to monitor the vertical profile of particle surface and number concentration above a major motorway. Diffusion chargers have been also used to directly characterize vehicle exhaust aerosols. Ntziachristos et al. (2004) showed that a diffusion charger calibrated with diesel aerosol can be used to obtain real-time particle surface recordings of exhaust emissions. Kittelson et al. (2005) combined two different models of diffusion chargers, a PAS and a CPC in a similar manner to Bukowiecki et al. (2002) to characterize vehicle exhaust instead of ambient concentrations. Finally, Mohr et al. (2005) evaluated 16 instruments of different operation principles, including two different diffusion chargers, as candidates for vehicle PM emission certification. They concluded that, if a type-approval test can be based on any metric other than just particle mass, the instruments of choice would be the CPC or the diffusion chargers due to their excellent sensitivity, simplicity (compared to the other instruments), repeatability and dynamic range. These studies make clear that diffusion chargers have a strong potential to be used alone as particle surface monitors or in combination with other instruments to provide information on particle properties, such as the mean surface diameter (combined with a CPC) or qualitative surface chemistry characteristics (in combination with a PAS), in real time.

Based on these promising results, we apply two diffusion chargers of the same model in this study (NSAM, TSI Model 3550) to monitor the particle surface concentration in urban environments where different particle levels and characteristics are expected. These environments include: (a) a retirement community (where both indoor and outdoor PM was monitored), (b) a typical downtown urban site, and (c) a freeway with significant heavy-duty diesel vehicle traffic. All sites were located in the Los Angeles Basin. The NSAM signal was also combined with the CPC number concentration to come up with a mean surface diameter.

2. METHODS

2.1. Instrumentation

The two diffusion chargers used in this study were of the same model (NSAM; Model 3550, TSI Inc., Shoreview, MN), developed by Fissan et al. (2007). Particle number concentrations were measured with either water-type (W-CPC; Model 3785, TSI Inc., Shoreview, MN) or butanol-type (CPC; Model 3022-A, TSI Inc., Shoreview, MN) CPCs. These instruments count particles down to 5 nm and 6 nm, respectively. The W-CPCs have been shown to satisfactorily correlate with butanol-type CPCs at ambient background number concentrations, e.g., up to $40,000 \text{ cm}^{-3}$ (Biswas et al. 2005). Finally, a Scanning Mobility

Particle Sizer (SMPS, model 3936L, TSI Inc., Shoreview, MN) was used to measure particle size distributions in the mobility range 16–638 nm every 120 s, with a sample flowrate of 0.3 l min⁻¹ and a sheath flowrate of 3.0 l min⁻¹.

In the NSAM a corona discharge produces ions, which are swept by a by-pass flow. A subsonic orifice accelerates the flow and forms a turbulent jet, which opposes a similar jet of aerosol particles formed by a second subsonic orifice. Particles are charged in the mixing zone of the two opposing jets (Medved et al. 2000). After charging, particles are collected on a filter and an electrometer measures the current produced as they release their charge. An electrostatic precipitator upstream of the filter, operating at moderate voltage, traps ions that escape the charging zone. For a monodisperse aerosol of concentration N (cm⁻³) the current produced as particles are collected on the filter is given by:

$$I = eQN\eta n_q \quad [1]$$

In Equation (1), e is the electronic charge ($e = 1.6 \times 10^{-19}$ coulomb), $Q = 1.5$ l min⁻¹ is the aerosol sample flowrate, η is the particle penetration through the device and n_q is the mean number of elementary charges per particle.

For a polydisperse aerosol, Equation (1) needs to be integrated over the NSAM size range, substituting the number concentration (N) with the number size distribution as a function of particle diameter. Both η and n_q depend on particle size and are determined by instrument calibration (Shin et al. 2007). For NSAM operating in the so-called “alveolar” mode used in this study, a power fit to the experimental data above 10 nm leads to (where d_p is expressed as mobility-equivalent in nm):

$$\eta(d_p)n_q(d_p) = 0.01d_p^{1.258} \quad [2]$$

The NSAM response is similar to a previous version of the instrument (EAD; Kaufman et al. 2002) and similar to the charging efficiency as a function of particle size measured by Jung and Kittelson (2005), Marjamäki et al. (2000), Ntziachristos et al. (2004), and Biskos et al. (2005) for particles in the transition regime (roughly 50–300 nm). Obviously, the exact response depends on a number of factors, including ion concentration, residence time of particles in the charger, particle losses and particle agglomeration. However the response of all instruments follows the theory of ionic diffusion in the transition regime (Fuchs 1963), which associates elementary charges per particle and particle diameter with a power law in the form $n_q \propto d_p^x$, where $1 < x < 2$.

The upper size limit of NSAM is determined by an inlet cyclone with $d_{50\%} = 1$ μ m aerodynamic diameter. The lower limit cannot be explicitly defined, as both η and n_q are functions of particle size, approaching zero as particle size decreases. According to the instrument specifications, the lower detection limit is 10 nm. Assuming that the response in Equation (2) is accurate down to 10 nm, the limit of detection of the NSAM

electrometer (0.1 fA) corresponds to ~ 130 cm⁻³ particles at 10 nm.

The total particle surface concentration is calculated by means of Equation (3), where k an instrument-specific calibration constant (Shin et al. 2007).

$$S_A = kI \quad [3]$$

Based on Fissan et al. (2007), the surface calculated by Equation (3) corresponds to the geometric surface of particles depositing in the alveolar region of the human respiratory tract (Wilson et al. 2004).

As Bukowiecki et al. (2002) demonstrated, the diffusion charger response and the total particle number concentration, measured for example by a CPC, can be combined to estimate the mean surface diameter (d_S). This can be done by combining Equations (1) to (3), to obtain:

$$d_S = \left(\frac{S_A}{0.01keQN} \right)^{1/1.258} \quad [4]$$

Following the definition of each moment average, d_S corresponds to the mobility diameter of a monodisperse aerosol with the same surface and number concentration of the actual aerosol.

The two NSAMs and the two W-CPCs were tested at the University of Southern California (USC) lab before being deployed in the field and showed high internal precision (R^2 of 0.99 and 0.98 for surface area and particle number concentration, respectively). In addition, the absolute levels measured by the two NSAMs agreed within 1% while CPC levels differed by 8%. No correction was applied to their signals, though, since this difference was within the manufacturer’s error margins ($\pm 10\%$).

2.2. Sampling Sites and Periods

Particle surface and number concentration were monitored in various environments in order to provide information for exposure to PM surface in different urban locations. Table 1 provides a summary of the sampling periods and the instruments used in each location.

The first site was a retirement community (RC) located about 5 miles east of downtown Los Angeles, approximately 0.1 mile south of a major freeway (I-10) and represents a typical residential location. Two identical sampling stations were installed here, one indoors and one outdoors. The indoor station was situated in the dining room of the community’s main building where cooking activities, which regularly occurred between 6:00 and 9:00 in the morning, were shown to be the major indoor sources of PM_{2.5} throughout the year (Polidori et al. 2007). The average air exchange rate was quite low at this location (0.31 h⁻¹ \pm 0.10 for winter), which is consistent with the structural characteristics of the sampling site (a dining hall in the middle of the retirement homes), the low number of open windows and doors, and the presence of central air conditioners. The outdoor station, set-up

TABLE 1
Sampling sites, time periods and instrumentation available at each site

Sampling site	Time period (Year 2006)	Instruments
RC Indoor	Jan. 5–Jan. 31	Model 3550 NSAM Model 3785 CPC
RC Outdoor	Jan. 5–Jan. 31	Model 3550 NSAM Model 3785 CPC
USC	Mar. 14–Apr. 19	Model 3550 NSAM Model 3785 CPC Model 3936L SMPS
I-710 FWY	Feb. 21–Apr. 4	Model 3550 NSAM Model 3022A CPC Model 3936L SMPS
I-710 BG	Feb. 22–Mar. 9	Model 3550 NSAM

RC = Retirement community; USC: University of Southern California; FWY = Freeway; BG = Background.

inside a mobile trailer, was located within 300 m of the indoor sampling area. Two NSAM devices and two W-CPC (operating flowrate = 1 l min^{-1} – $d_{50\%}$ cutpoint at 5 nm) were operated concurrently indoors and outdoors.

The second site was located at the campus of the University of Southern California (USC). This site is about 100 m downwind of a major (mainly gasoline vehicle) freeway and just south of downtown Los Angeles. The ambient air at this site represents a typical urban mix of mobile, industrial, and construction sources (Sardar et al. 2005). Here, an NSAM, a W-CPC, and an SMPS operated continuously. All instruments were installed inside a stationary trailer and ambient samples were drawn from inlets located on the trailer roof.

Finally, particle number and surface measurements were conducted at two different locations, influenced by the I-710 freeway. This is a 26 m wide, eight-lane highway connecting the ports complex of Long Beach and San Pedro to the shipping yards in east Los Angeles. The vehicle density during the sampling period was 10,000–11,000 vehicles h^{-1} with a heavy-duty diesel vehicle fraction of $\sim 18\%$ on average. More information on the traffic profile during sampling is provided by Ntziachristos et al. (2007). The first location was directly adjacent to the I-710 with the sampling probe inlet located approximately 10 m from the freeway shoulder. The sampling station was set-up inside a truck that was driven to the site daily, while samples were typically collected between 11:00 and 19:00. Copper tubes were extended approximately one meter above the truck's roof to collect aerosol samples. An NSAM, an SMPS, and a CPC were deployed at this site. A similar measurement station was also set up approximately 100 m downwind of the freeway on a bike path parallel to the Los Angeles River, to sample a more atmospherically "aged" aerosol. This site was thus considered representative of background particle levels that are still influenced by the freeway. Its location/distance with respect to the

freeway was based on the work of Zhu et al. (2002), who showed that particle levels reached almost urban background levels at a 100–150 m distance downwind of a freeway.

3. RESULTS AND DISCUSSION

3.1. Particle Number and Surface Concentration in Different Locations

Table 2 presents the mean particle surface and number concentrations measured with the NSAM and CPC, respectively, at the five different sampling sites. The total number of hourly samples is also reported for each location. Mean values correspond to continuous 24 h sampling for all locations, except the site in proximity of I-710, where sampling took place only between 11:00–19:00. The variance in the mean concentration is expressed by means of the standard deviation over the entire sampling period. The highest number and surface levels were recorded next to the I-710 freeway, due to the proximity of this site to vehicle emissions. Surface concentrations remained relatively high at the I-710 background site, which is located about 100 m downwind of the freeway. On the other hand, surface and number concentrations at the urban background (USC) and the RC sites were much lower than at locations directly affected by emissions from the I-710 freeway.

The ranges of variance presented in Table 2 are better explained by examining the diurnal profile of surface and particle number concentrations in Figures 1 and 2, respectively. We first focus on the time evolution of surface and number concentrations next to the I-710 freeway. Both surface and number concentrations increase as the day progresses from late morning to the afternoon. In particular, the surface concentration peaks at 16:00 while the number rather monotonically increases in the afternoon. Ntziachristos et al. (2007) demonstrated that black carbon and particle volume in the accumulation mode (40–638 nm) also peaked at 16:00. During this time, the mean vehicle speed in the freeway reaches its lowest value (75 km/h compared to an average of 83 km/h), as a result of the afternoon rush hour. As traffic density decreases later in the evening, the surface (along with black carbon and volume of particles) decreases. Therefore, the local peak in particle surface concentration can be associated to relatively heavy traffic conditions. However, the number concentration continues to grow through the early evening hours, as a result of the decrease in ambient temperature (e.g., from an average of 22.7°C at 13:00 to 13.4°C at 18:00), which promotes the formation of nanoparticles by condensation of organic vapors from vehicle exhaust.

In all sites where 24 h sampling was conducted, a local peak appears between 6:00–8:00, which coincides with the morning rush hour. The surface concentration then drops during mid-day and increases again in the evening, forming a second local peak between 23:00 and 1:00. The particle number concentration seems to follow a similar pattern for both urban outdoor (RC and USC) sites. In the absence of any known urban sources whose activity becomes maximum during the overnight time

TABLE 2
Mean particle surface (NSAM) and number (CPC) concentrations measured at different sampling sites

Sampling site	Daily sampling duration	Total hourly samples	NSAM Surface ($\mu\text{m}^2 \text{cm}^{-3}$)		CPC concentration (cm^{-3})	
			Mean	Standard deviation	Mean	Standard deviation
RC Indoor	24 h	557	45.2	26.1	12938	4094
RC Outdoor	24 h	630	68.9	38.7	18448	6049
USC	24 h	356	53.0	27.5	14676	5808
I-710 BG	24 h	124	105.8	48.3	Not measured	
I-710 FWY	11:00–19:00	159	153.4	55.2	93015	56607

period, the surface increase is likely due to new particle formation by nucleation as well as condensational particle growth as the temperature drops and the atmospheric mixing height decreases during that period.

It is also interesting to compare the diurnal profile of surface and number concentrations between the outdoor and the indoor RC sites. The morning rush hour event seems to affect the outdoor site. However, at the same time (6:00–9:00 in the morning), substantial peaks appear both in number and surface of indoor particle concentrations, which by far exceed the outdoor increase. Those peaks are a strong indication of an indoor

source, and most likely are related to morning cooking activities in the kitchen adjacent the indoor sampling site where all meals of the day were cooked at this time by using gas stoves/ovens. With the exception of these local peaks due to cooking, the magnitudes and trends of indoor and outdoor particle concentrations closely track each other, with indoor levels always lower than outdoor levels, which suggest that the majority of indoor particles in that site originate from outdoors. This is also confirmed by the findings of a recent study conducted at the same RC and during the same time period (Polidori et al. 2007), which showed that outdoor sources of $\text{PM}_{2.5}$ and its carbonaceous components (e.g., organic and elemental carbon) are the most important contributors to the indoor PM levels.

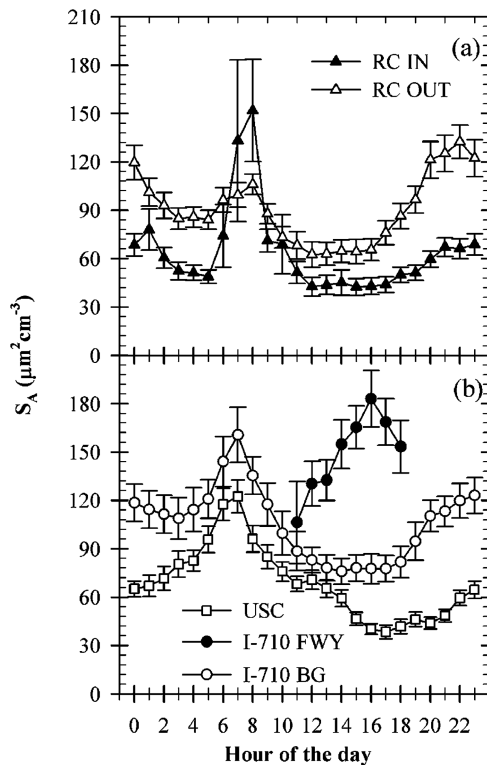


FIG. 1. Temporal variation of the particle surface concentration measured with the NSAM at (a) Indoors (IN) and outdoors (OUT) of a retirement community and, (b) an urban background site (USC) and a proximal (FWY) and a distant (BG) site to the I-710 freeway.

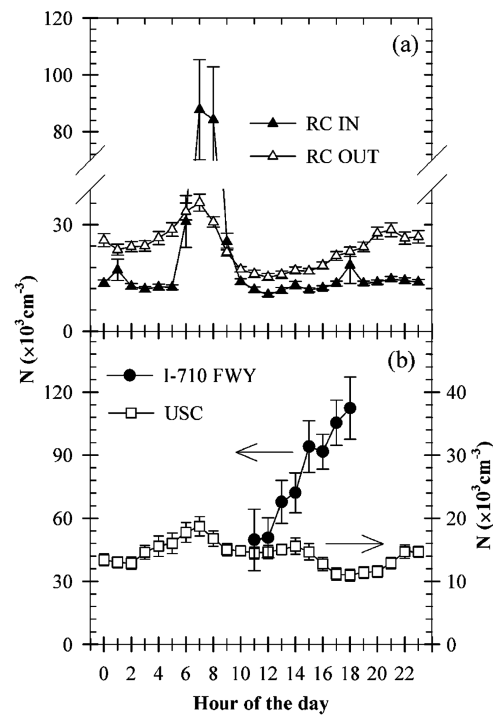


FIG. 2. Temporal variation of the particle number concentration at different sampling sites, measured with the CPC. Acronyms in legend are similar to Figure 1.

3.2. Mean Surface Diameter

The diurnal profile of the mean surface diameter (d_s), calculated according to Equation (4), is shown in Figure 3 for the different sampling sites. At the RC sites, the mean diameters indoors and outdoors track each other well during the day, except when cooking activities were taking place (6:00–9:00). During that time, a large number of small particles is produced indoors, which leads to an increase in the surface concentration. In general, d_s increases both indoors and outdoors in the evening as the temperature drops, which, as argued earlier, is probably due to condensational growth of the particles at that time. However, the mean indoor diameter is always slightly lower than the outdoor (except between 3:00–5:00), which may be due to some particle evaporation as the aerosol is transported in the warmer indoor environment (Kuhn et al. 2005; Lunden et al. 2003; Sarnat et al. 2006). For example, particulate compounds such as ammonium nitrate and organic species, which may account for 35–60% of outdoor $PM_{2.5}$ mass in the Los Angeles basin (Kim et al. 2000; Tolocka et al. 2001), volatilize as they entrain indoors (Lunden et al. 2003).

The comparison between the freeway and the urban background site reveals that the mean surface diameter is somewhat smaller next to the freeway, but there is generally very good agreement between the trends of the background and the freeway concentrations. During late afternoon (after 17:00) d_s next

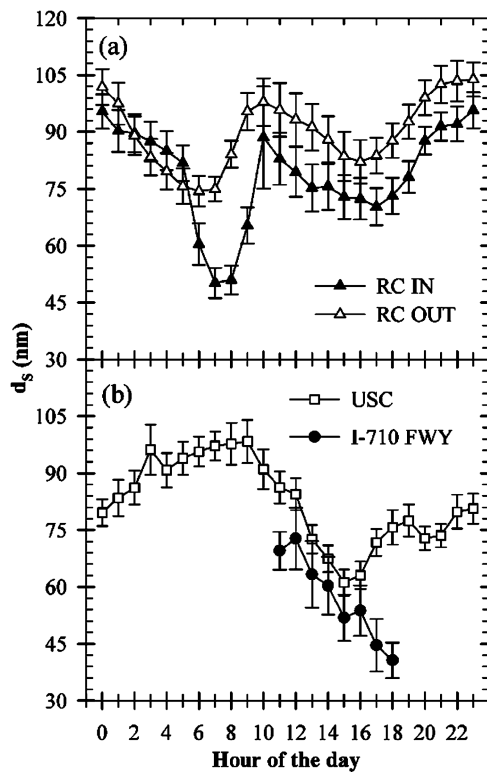


FIG. 3. Temporal variation of the mean surface diameter obtained by combination of the NSAM and the CPC concentrations. Acronyms in legend are similar to Figure 1.

to the freeway decreases to below 40 nm, indicating the formation of a significant number of fresh nanoparticles by nucleation.

3.3. NSAM Performance Validation

The comparison of the mean surface diameter calculated by NSAM and CPC with the arithmetic average (\bar{d}_p) obtained from the SMPS distributions may be used as a validation of the NSAM operation and a measure of consistency between NSAM/CPC and SMPS. The surface mean diameter is the 1.258-moment average of mobility diameter and one should expect it to be in the same range, but larger, than the arithmetic mean. This comparison is shown in Figure 4 for the two locations where SMPS measurements were available. It should be restated that the USC site is representative of urban background aerosol while the I-710 is representative of fresh vehicular aerosol, including a large fraction of diesel exhaust. It should also be noted that \bar{d}_p corresponds to the 16–638 nm mobility range while d_s , although expressed as mobility equivalent, corresponds to the more vaguely defined size range of NSAM, i.e., to particles between ~ 10 nm in mobility diameter to $1 \mu\text{m}$ in aerodynamic diameter. Despite the different size ranges and surface definitions, there is a good correlation ($R^2 = 0.67$) between the two diameter expressions at USC (Figure 4a) for the 356 hourly samples considered. The grand average of all mean surface and arithmetic diameters is 86 nm and 59 nm, respectively. This is consistent with the expression of surface as a larger than one moment of mobility

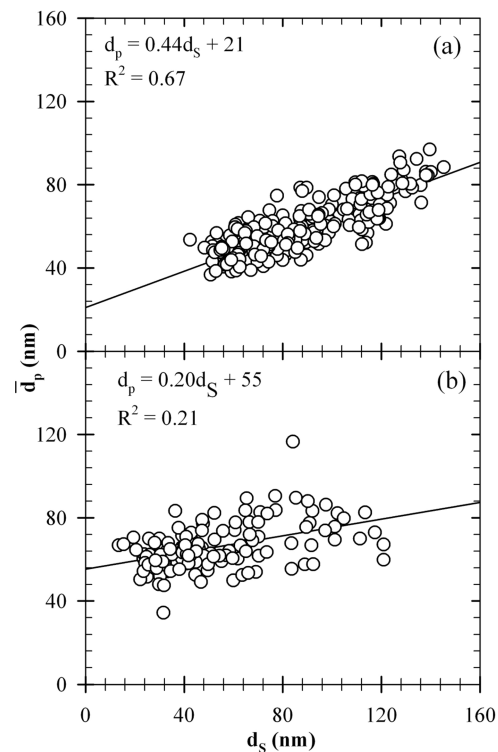


FIG. 4. Correlation between the arithmetic average (\bar{d}_p) and mean surface (d_s) diameters at (a) the USC and (b) the I-710 FWY sampling sites.

diameter. Therefore, these results suggest that the mean surface diameter is a good indicator of the average aerosol size at an urban background location. In addition, this parameter can be derived in much faster time intervals than the SMPS mean diameter.

The correlation was not as satisfactory ($R^2 = 0.21$) next to the freeway (Figure 4b), with \bar{d}_p varying in the range ~ 50 – 90 nm and d_S reaching sizes as low as 20 nm for the 159 hourly samples collected in total. Since it is physically impossible that the mean surface diameter be smaller than the mean arithmetic diameter, this reveals some inconsistency between the NSAM and SMPS measurements. To further investigate the reasons for this inconsistency, we compared the absolute levels of surface concentration measured by NSAM to the total equivalent surface corresponding to the SMPS distributions. The latter can be calculated by using the SMPS number size distribution as an input to Equation (1) and summing up over all SMPS size bins to calculate the total equivalent current assumed by the distribution, and then estimate the equivalent surface ($S_{A,SMPS}$) by means of Equation (3). The correlation of S_A and $S_{A,SMPS}$ is shown in Figure 5 for the two sampling locations. The correlation coefficient ($R^2 = 0.94$) and the slope (0.87) at USC are both indicative of very good agreement between the two methods, consistent with the good correlation observed for the mean diameters shown in Figure 4a. On the other hand, the slope of the linear regression of $S_{A,SMPS}$ vs. S_A is 0.42 and the correlation coefficient is much lower ($R^2 = 0.64$) next to the I-710 (Figure 5b) than at USC.

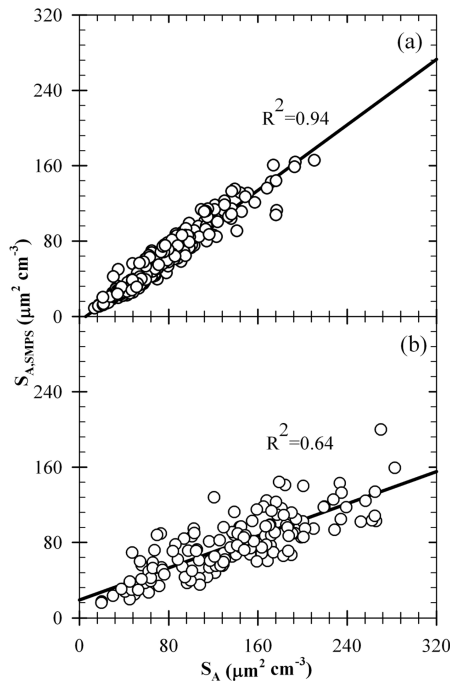


FIG. 5. Correlation between the equivalent surface concentration corresponding to the SMPS size distribution ($S_{A,SMPS}$) and the NSAM surface (S_A) for (a) the USC and (b) the I-710 FWY sampling sites.

The reasons for the discrepancy between NSAM and SMPS equivalent surfaces, and in particular the difference in the degree of correlation at the two locations, could be explored by studying the surface distribution as a function of particle size in each location to determine whether the different levels are due to the surface of particles outside the SMPS size range (16 – 638 nm). Figure 6 compares the surface distribution as a function of size next to the I-710 and at USC for two different hours of the day ($13:00$ and $18:00$). The late afternoon hour was selected because, as discussed in Figure 2, a large number of nanoparticles forms next to the I-710 as the temperature drops in the evening, and this leads to a bi-modal number distribution with large particle concentration below 40 nm (nucleation mode) (Ntziachristos et al. 2007). The NSAM particle surface decreased from $65.5 \mu\text{m}^2 \text{cm}^{-3}$ to $41 \mu\text{m}^2 \text{cm}^{-3}$ between $13:00$ to $18:00$ at USC (Figure 1b). Integration of the size distributions in Figure 6 reveals a similar drop in SMPS equivalent surface, from $51 \mu\text{m}^2 \text{cm}^{-3}$ to $28 \mu\text{m}^2 \text{cm}^{-3}$. The $\sim 30\%$ higher NSAM levels could be attributed to the particle surface missed by the SMPS below 16 nm and above 638 nm.

Next to the I-710 freeway, the NSAM surface concentration increases from $133 \mu\text{m}^2 \text{cm}^{-3}$ at $13:00$ to $153 \mu\text{m}^2 \text{cm}^{-3}$ at $18:00$ (Figure 1b). However, the SMPS equivalent surface decreases from $93 \mu\text{m}^2 \text{cm}^{-3}$ to $76 \mu\text{m}^2 \text{cm}^{-3}$. The SMPS equivalent surface at $13:00$ is $\sim 30\%$ lower than the NSAM, as in the case of USC. However, the SMPS surface area at $18:00$ is at least 50% lower than the corresponding NSAM. Figure 6b

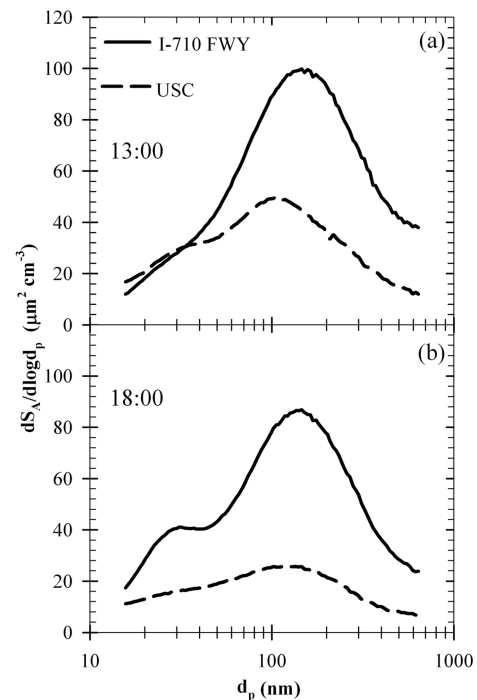


FIG. 6. Hourly average surface size distributions at the USC and I-710 FWY, corresponding to (a) $13:00$ and (b) $18:00$.

shows that there is a significant particle surface concentration associated with sub-40 nm particles at 18:00 next to the freeway. Therefore, the surface of nanoparticles (<16 nm) not sampled by the SMPS might be responsible for this deviation. In an effort to reconcile the SMPS-equivalent with the NSAM surface concentrations, Table 3 shows the SMPS (16–638 nm) and the CPC (>6 nm) number concentrations in the two locations and different sampling hours, including the cases discussed in Figure 6. It is reasonable to assume that the difference in the CPC and SMPS number concentrations is due to particles smaller than 16 nm and nanoparticles lost in the DMA by diffusion (Birmili et al. 1997). Using a different SMPS configuration that allowed particle measurements down to 6 nm in mobility diameter, Zhu et al. (2004) showed that the peak in the number concentration next to the I-710 freeway was at about 10 nm in the wintertime. We thus assumed that the size distribution of particles not captured by SMPS is centered around 10 nm mobility diameter, which is also the lower NSAM detection limit considered by the manufacturer. This diameter value and the difference in the CPC and SMPS concentrations were used as inputs to Equation (1) to calculate the NSAM current carried by these particles. Their equivalent surface is then calculated by means of Equation (3). According to the NSAM calibration provided by Shin et al. (2007), the assumption to use an average instrument response at 10 nm is a reasonable approximation for sub-16 nm

particles. The exact response depends on the size distribution below 16 nm, which is not available.

The results of this procedure are shown in Table 3 for both the PIU and I-710 sites. The table also distinguishes between particles in the size ranges 16–40 nm and 40–638 nm, which are both measured by the SMPS. Finally, the last column gives the ratio of the SMPS-equivalent and sub-16 nm surface concentration over the NSAM surface concentration. The mean contribution of the three particle classes (<16 nm, 16–40 nm and 40–640 nm) is 22%, 11%, and 67%, respectively, at the freeway and 10%, 19%, and 71%, respectively, at USC. These results not only show that the surface area concentration next to the freeway is larger than in an urban background site, but that the relative contribution of nanoparticles to the total aerosol surface is much higher as well.

The last column in Table 3 shows that the reconstructed surface concentration, with the inclusion of particles less than 16 nm, can explain 70–90% of the NSAM concentration next to the freeway and 84% of the concentration at the urban background site. Obviously, a large fraction of the unexplained surface area may originate from particles >638 nm. Additionally, the calculation of the surface concentration in the <16 nm range is confounded by the uncertainty in the estimation of the mean particle size in this range. Assuming a somewhat larger mean particle diameter for these particles would further reduce the difference

TABLE 3
Comparison of the NSAM and reconstructed hourly average surface concentrations next to the I-710 freeway and at an urban background site (USC)

Hour	NSAM ($\mu\text{m}^2 \text{cm}^{-3}$)	SMPS (cm^{-3})	CPC (cm^{-3})	Reconstructed surface concentration ($\mu\text{m}^2 \text{cm}^{-3}$)				Total reconstructed/NSAM Surface ratio
				<16 nm	16–40 nm	40–638 nm	Total	
I-710 FWY								
11:00	106	16567	49745	14	12	71	96	0.90
12:00	130	14809	50699	15	10	86	111	0.85
13:00	133	16349	67764	22	10	83	115	0.87
14:00	155	18155	72187	23	12	88	123	0.79
15:00	165	20057	94090	31	12	83	126	0.76
16:00	183	22661	91695	29	16	89	134	0.73
17:00	169	19907	105382	36	14	70	120	0.71
18:00	153	18235	112418	39	14	62	115	0.75
USC								
11:00	68	10583	14164	3	9	46	57	0.84
12:00	71	12034	16999	4	11	44	59	0.83
13:00	65	11717	17362	5	11	40	56	0.85
14:00	59	10772	17156	5	11	34	49	0.83
15:00	47	9057	14841	5	9	27	40	0.87
16:00	40	7327	13331	5	7	23	35	0.86
17:00	38	6680	11929	4	6	22	33	0.85
18:00	42	6765	11944	4	6	22	33	0.79

between the reconstructed concentration and the NSAM. Finally, part of the difference could be associated with uncertainties in the NSAM response (Equation [2]). This is particularly important for soot agglomerate particles next to the freeway in the size range above ~ 200 nm, which may be charged with even higher efficiency than what Equation (2) suggests. Nonetheless, the fact that the absolute value of the reconstructed/NSAM ratio is close to unity and that it varies only within the range of 0.7–0.9 is a very good indication of the consistency in the measurements of the NSAM, SMPS, and CPC.

4. SUMMARY AND CONCLUSIONS

Two NSAM units were used to measure the ambient particle surface concentrations and their diurnal profiles in different environments. The sampling sites included a freeway heavily influenced by heavy-duty diesel traffic, an urban background monitoring station and a retirement community. At the freeway location, samples were taken immediately next to the freeway shoulder and at a station located 100 m downwind. At the retirement community, both outdoor and indoor measurements were concurrently conducted. The NSAM surface and CPC number concentrations were combined to derive the mean surface diameter, which was then compared to the mean arithmetic diameter obtained by SMPS distributions.

Measurements show that the particle surface concentration decreased as we moved from the proximity of the freeway to the freeway background, then to the urban background sites and, finally, indoors. The diurnal profile of the particle surface concentration shows that in all sites (except next to the 710 freeway where no data were available) the concentrations peaked in the early daytime hours (7:00–8:00), reflecting the effect of increased traffic activity. For the indoor concentrations, indoor sources (mainly cooking) also become a significant contributor to the particle surface area in these morning hours. Next to the freeway, data were only available between 11:00 to 18:00 and showed that the peak surface concentration was observed during the afternoon rush hour (16:00).

The mean surface diameter at the retirement community shows a strong diurnal profile both indoors and outdoors. The largest mean surface diameters appear in the late night–early morning hours, presumably as a result of condensational growth during these relatively low temperature conditions. The mean surface diameters were significantly lower both outdoors and in particular indoors in the early daytime hours due to fresh aerosol produced by a nearby freeway and indoor (cooking) activities, respectively. The indoor mean diameter remained lower than the outdoor throughout nearly the entire 24 h sampling.

The mean surface diameter in the range 10 nm–1 μm measured by the NSAM-CPC was satisfactorily correlated ($R^2 = 0.67$) to the arithmetic average diameter determined by the SMPS (range 16–638 nm) at the urban background site but was much less correlated ($R^2 = 0.21$) next to the freeway. Comparison of the NSAM with the equivalent surface concentration

of SMPS size distributions revealed that the lack of correlation next to the freeway should be at least in part attributed to the surface area of sub-16 nm particles, which are not measured by the SMPS. We estimated that the surface area of these smaller particles could be as much as 34% of the total surface concentration, which has significant implications to particle exposure next to the freeway.

This study confirms earlier evidence that diffusion chargers are useful and reliable instruments for measuring ambient aerosol concentrations in different environments and that their signal can be combined with the CPC number concentration to provide an estimate of the mean particle diameter in real time.

REFERENCES

- Birmili, W., Stratmann, F., Wiedensohler, A., Covert, D., Russell, L. M., and Berg, O. (1997). Determination of Differential Mobility Analyzer Transfer Functions Using Identical Instruments in Series, *Aerosol Sci. Technol.* 27: 215–223.
- Biskos, G., Reavell, K., and Collings, N. (2005). Unipolar Diffusion Charging of Aerosol Particles in the Transition Regime, *J. Aerosol Sci.* 36:247–265.
- Biswas, S., Fine, P. M., Geller, M. D., Hering, S. V., and Sioutas, C. (2005). Performance Evaluation of a Recently Developed Water-Based Condensation Particle Counter, *Aerosol Sci. Technol.* 39:419–427.
- Brown, D. M., Wilson, M. R., MacNee, W., Stone, V., and Donaldson, K. (2001). Size-Dependent Proinflammatory Effects of Ultrafine Polystyrene Particles: A Role for Surface Area and Oxidative Stress in the Enhanced Activity of Ultrafines, *Toxicol. Appl. Pharmacol.* 175:191–199.
- Bukowiecki, N., Kittelson, D. B., Watts, W. F., Burtcher, H., Weingartner, E., and Baltensperger, U. (2002). Real-Time Characterization of Ultrafine and Accumulation Mode Particles in Ambient Combustion Aerosols, *J. Aerosol Sci.* 33:1139–1154.
- Elder, A., Gelein, R., Finkelstein, J. N., Driscoll, K. E., Harkema, J., and Oberdörster, G. (2005). Effects of Subchronically Inhaled Carbon Black in Three Species. I. Retention Kinetics, Lung Inflammation, and Histopathology, *Toxicol. Sci.* 88:614–629.
- Fissan, H., Neumann, S., Trampe, A., Pui, D. Y. H., and Shin, W. G. (2007). Rationale and Principle of an Instrument Measuring Lung Deposited Nanoparticle Surface Area, *J. Nanopart. Res.* 9:53–59.
- Fuchs, N. A. (1963). On the Stationary Charge Distribution on Aerosol Particles in a Bipolar Ionic Atmosphere, *Geofisica Purae Applicata* 56:185–193.
- Gäggeler, H. W., Baltensperger, U., Emmenegger, M., Jost, D. T., Schmidt-Ott, A., Haller, P., and Hofmann, M. (1989). The Epiphaniometer, a New Device for Continuous Aerosol Monitoring, *J. Aerosol Sci.* 20:557–564.
- Imhof, D., Weingartner, E., Vogt, U., Dreiseidler, A., Rosenbohm, E., Scheer, V., Vogt, R., Nielsen, O. J., Kurtenbach, R., Corsmeier, U., Kohler, M., and Baltensperger, U. (2005). Vertical Distribution of Aerosol Particles and NO_x Close to a Motorway, *Atmos. Environ.* 39:5710–5721.
- Jung, H. J. and Kittelson, D. B. (2005). Characterization of Aerosol Surface Instruments in Transition Regime, *Aerosol Sci. Technol.* 39:902–911.
- Kaufman, S. L., Medved, A., Pöcher, A., Hill, N., Caldow, R., and Quant, F. R. (2002). An Electrical Aerosol Detector Based on the Corona-Jet Charger, in *Abstracts of the 21st annual AAAR Conference*, Charlotte, NC, p. 223.
- Kim, B. M., Teffera, S., and Zeldin, M. D. (2000). Characterization of $\text{PM}_{2.5}$ and PM_{10} in the South Coast Air Basin of Southern California: Part 1-Spatial Variations, *J. Air & Waste Manage. Assoc.* 50:2034–2044.
- Kittelson, D. B., Watts, W. F., Savstrom, J. C., and Johnson, J. P. (2005). Influence of a Catalytic Stripper on the Response of Real Time Aerosol Instruments to Diesel Exhaust Aerosol, *J. Aerosol Sci.* 36:1089–1107.

- Kuhn, T., Krudysz, M., Zhu, Y. F., Fine, P. M., Hinds, W. C., Froines, J., and Sioutas, C. (2005). Volatility of Indoor and Outdoor Ultrafine Particulate Matter near a Freeway, *J. Aerosol Sci.* 36:291–302.
- Lunden, M. M., Revzan, K. L., Fischer, M. L., Thatcher, T. L., Littlejohn, D., Hering, S. V., and Brown, N. J. (2003). The Transformation of Outdoor Ammonium Nitrate Aerosols in the Indoor Environment, *Atmos. Environ.* 37:5633–5644.
- Marjamäki, M., Keskinen, J., Chen, D. R., and Pui, D. Y. H. (2000). Performance Evaluation of the Electrical Low-Pressure Impactor (ELPI), *J. Aerosol Sci.* 31:249–261.
- Matter, U., Siegmann, H. C., and Burtscher, H. (1999). Dynamic Field Measurements of Submicron Particles from Diesel Engines, *Environ. Sci. Technol.* 33:1946–1952.
- Maved, A., Dorman, F., Kaufman, S. L., and Pöcher, A. (2000). A New Corona-Based Charger for Aerosol Particles, *J. Aerosol Sci.* 31:S616–S617.
- Mohr, M., Lehmann, U., and Rutter, J. (2005). Comparison of Mass-Based and Non-Mass-Based Particle Measurement Systems for Ultra-Low Emissions from Automotive Sources, *Environ. Sci. Technol.* 39:2229–2238.
- Moshhammer, H. and Neuberger, M. (2003). The Active Surface of Suspended Particles as a Predictor of Lung Function and Pulmonary Symptoms in Austrian School Children, *Atmos. Environ.* 37:1737–1744.
- Ntziachristos, L., Giechaskiel, B., Ristimäki, J., and Keskinen, J. (2004). Use of a Corona Charger for the Characterisation of Automotive Exhaust Aerosol, *J. Aerosol Sci.* 35:943–963.
- Ntziachristos, L., Ning, Z., Geller, M. D., and Sioutas, C. (2007). Particle Concentration and Characteristics near a Major Freeway with Heavy-Duty Diesel Traffic, *Environ. Sci. Technol.*: In press.
- Oberdörster, G. (2001). Pulmonary Effects of Inhaled Ultrafine Particles, *Intl. Arch. Occupat. Environ. Health* 74:1–8.
- Pandis, S. N., Baltensperger, U., Wolfenbarger, J. K., and Seinfeld, J. H. (1991). Inversion of Aerosol Data from the Epiphaniometer, *J. Aerosol Sci.* 22:417–428.
- Polidori, A., Arhami, M., Delfino, R. J., and Sioutas, C. (2007). Indoor/Outdoor Relationships, Trends and Carbonaceous Content of Fine Particulate Matter in Retirement Homes of the Los Angeles Basin, *J. Air & Waste Manage. Assoc.*: In press.
- Pui, D. Y. H., Fruin, S., and McMurry, P. H. (1988). Unipolar Diffusion Charging of Ultrafine Aerosols, *Aerosol Sci. Technol.* 8:173–187.
- Rogak, S. N. and Flagan, R. C. (1992). Bipolar Diffusion Charging of Spheres and Agglomerate Aerosol-Particles, *J. Aerosol Sci.* 23:693–710.
- Sardar, S. B., Fine, P. M., and Sioutas, C. (2005). Seasonal and Spatial Variability of the Size-Resolved Chemical Composition of Particulate Matter (PM10) in the Los Angeles Basin, *J. Geophys. Res.-Atmospheres* 110.
- Sarnat, S. E., Coull, B. A., Ruiz, P. A., Koutrakis, P., and Suh, H. H. (2006). The Influences of Ambient Particle Composition and Size on Particle Infiltration in Los Angeles, Ca, Residences, *J. Air & Waste Manage. Assoc.* 56:186–196.
- Shin, W. G., Pui, D. Y. H., Fissan, H., Neumann, S., and Tramp, A. (2007). Calibration and Numerical Simulation of Nanoparticle Surface Area Monitor (TSI Model 3550 NSAM), *J. Nanopart. Res.* 9:61–69.
- Siegmann, K. and Siegmann, H. C. (2000). Fast and Reliable “in-Situ” Evaluation of Particles and Their Surface with Special Reference to Diesel Exhaust, *SAE Technology Paper*: 2000-01-1995.
- Sinclair, A. H. and Tolsma, D. (2004). Associations and Lags between Air Pollution and Acute Respiratory Visits in an Ambulatory Setting: 25-Month Results from the Aerosol Research and Inhalation Epidemiology Study (Aries), *J. Air & Waste Manage. Assoc.* 54:1212–1218.
- Stoeger, T., Reinhard, C., Takenaka, S., Schroepel, A., Karg, E., Ritter, B., Heyder, J., and Schulz, H. (2006). Instillation of Six Different Ultrafine Carbon Particles Indicates a Surface Area Threshold Dose for Acute Lung Inflammation in Mice, *Environ. Health Perspect.* 114:328–333.
- Tolocka, M. P., Solomon, P. A., Mitchell, W., Norris, G. A., Gemmill, D. B., Wiener, R. W., Vanderpool, R. W., Homolya, J. B., and Rice, J. (2001). East Versus West in the U.S.: Chemical Characteristics of PM2.5 during the Winter of 1999, *Aerosol Sci. Technol.* 34:88–96.
- Tran, C. L., Buchanan, D., Cullen, R. T., Searl, A., Jones, A. D., and Donaldson, K. (2005). Inhalation of Poorly Soluble Particles. II. Influence of Particle Surface Area on Inflammation and Clearance, *Inhal. Toxicol.* 12:1113–1126.
- Wilson, W. E., Han, H. S., Stanek, J., Turner, J., Chen, D. R., and Pui, D. Y. H. (2004). Use of the Electrical Aerosol Detector as an Indicator for the Total Particle Surface Area Deposited in the Lung, in *Proceedings of the Annual Meeting of the Air & Waste Management Association*, Indianapolis, IN.
- Woo, K.-S., Chen, D.-R., Pui, D. Y. H., and Wilson, W. E. (2001). Use of Continuous Measurements of Integral Aerosol Parameters to Estimate Particle Surface Area, *Aerosol Sci. Technol.* 34:57–65.
- Zhu, Y., Hinds, W. C., Shen, S., and Sioutas, C. (2004). Seasonal and Spatial Trends in Fine Particulate Matter, *Aerosol Sci. Technol.* 38:5–13.
- Zhu, Y. F., Hinds, W. C., Kim, S., Shen, S., and Sioutas, C. (2002). Study of Ultrafine Particles near a Major Highway with Heavy-Duty Diesel Traffic, *Atmos. Environ.* 36:4323–4335.